HHS Public Access

Author manuscript

Ann Biomed Eng. Author manuscript; available in PMC 2017 March 01.

Published in final edited form as:

Ann Biomed Eng. 2016 March ; 44(3): 636–648. doi:10.1007/s10439-015-1515-0.

Quantitative Ultrasound for Nondestructive Characterization of Engineered Tissues and Biomaterials

Diane Dalecki[1], **Karla P. Mercado**[2], and **Denise C. Hocking**[3]

[1]Department of Biomedical Engineering University of Rochester, 310 Goergen Hall, P.O. Box 270168, Rochester, NY 14627, USA

[2]Department of Internal Medicine, University of Cincinnati, 231 Albert Sabin Way, Cincinnati, OH 45267, USA

[3]Department of Pharmacology and Physiology, University of Rochester, 601 Elmwood Avenue, Box 711, Rochester, NY 14642, USA

Abstract

Non-invasive, non-destructive technologies for imaging and quantitatively monitoring the development of artificial tissues are critical for the advancement of tissue engineering. Current standard techniques for evaluating engineered tissues, including histology, biochemical assays and mechanical testing, are destructive approaches. Ultrasound is emerging as a valuable tool for imaging and quantitatively monitoring the properties of engineered tissues and biomaterials longitudinally during fabrication and post-implantation. Ultrasound techniques are rapid, non-invasive, non-destructive and can be easily integrated into sterile environments necessary for tissue engineering. Furthermore, high-frequency quantitative ultrasound techniques can enable volumetric characterization of the structural, biological, and mechanical properties of engineered tissues during fabrication and post-implantation. This review provides an overview of ultrasound imaging, quantitative ultrasound techniques, and elastography, with representative examples of applications of these ultrasound-based techniques to the field of tissue engineering.

Keywords

Ultrasound; Imaging; Biomaterials; Tissue engineering; Elastography; Regenerative medicine

INTRODUCTION

A variety of illnesses and conditions, including infectious disease, trauma, and cancer, can lead to severe organ damage and tissue loss. In response, a major focus of the interdisciplinary field of tissue engineering has been to develop new approaches to either restore native tissue function or replace damaged tissues with functional tissue substitutes. To do so, various cell types are typically combined with either naturally derived or synthetic

Author to Whom Correspondence Should Be Addressed: Diane Dalecki, Ph.D., Department of Biomedical Engineering, 310 Goergen Hall, P.O. Box 270168, University of Rochester, Rochester, NY 14627 USA, dalecki@bme.rochester.edu.

CONFLICT OF INTEREST

No conflicts of interest exist.

scaffold materials to produce nascent three-dimensional (3-D) constructs. These constructs are subsequently exposed to a variety of chemical and biophysical stimuli to initiate key developmental processes, including cell proliferation, differentiation, and extracellular matrix deposition that mediate native tissue formation and maturation. Using various combinations of cells and biomaterials, attempts have been made to fabricate many different types of tissue.[1] Advancing the development and use of more complex tissues for clinical applications requires technologies that can characterize the properties of artificial constructs and regenerating tissues quantitatively, volumetrically, non-invasively, and non-destructively during fabrication, conditioning, and post-implantation.

To advance the field of tissue engineering, structural, biological, and functional characterizations of new tissue-engineered constructs must be performed in cell culture systems and animals models prior to testing in humans. Systematic evaluations of tissue constructs using standardized, quantitative methodologies would facilitate functional comparisons among different approaches and would accelerate clinical feasibility and acceptance. Currently, histology, immunohistochemistry, and direct mechanical tests are the most common techniques for evaluating engineered tissues and these techniques provide multiple avenues and metrics for characterizing biomaterials. Conventional histology combined with optical microscopy techniques are excellent for visualizing the microscopic anatomy of cells and the extracellular matrix. Direct mechanical testing methods, such as tensile and compression tests, can provide several quantitative measurements of a construct's mechanical properties, including elastic modulus, yield strength, and ultimate strength. Similarly, rheometry can provide bulk measurements of the viscoelastic properties of engineered tissues subjected to shear stresses and strains, while atomic force microscopy can be used to measure the elastic modulus and viscosity of biomaterial scaffolds and cell-embedded engineered tissues at the nanometer scale.

Although histology and direct mechanical tests have been used widely to characterize the structural and mechanical properties of engineered tissues, these techniques are destructive, and therefore, are incapable of monitoring changes in the properties of individual tissue constructs over time. Evaluating separate samples by histological and mechanical testing at multiple time points can be expensive and time-consuming. Furthermore, these techniques can only assess a small fraction of a larger volume of tissue, and thus, cannot evaluate engineered constructs volumetrically. Moreover, after implantation of the construct, biopsies are often required to assess the integration of engineered tissues with native tissues.

Non-invasive imaging technologies provide alternative tools to visualize and characterize materials.[2,3] Diagnostic imaging modalities, including X-ray, nuclear, magnetic resonance, and optical imaging, are currently employed to evaluate engineered tissues and biomaterials in vitro and in vivo.[2,3] No single modality is capable of imaging all tissue engineering applications (e.g., ranging from molecular imaging to imaging deep within tissue), and each has its own advantages and limitations.[2,3] Often several different imaging tools are employed (i.e. multi-modal imaging), exploiting the strengths of each individual technique, to provide complementary information to assess complex constructs.[3]

Ultrasound imaging is emerging as an important tool for tissue engineering applications because it provides non-invasive, non-destructive, real-time, qualitative and quantitative imaging capabilities. This paper presents an overview of ultrasound imaging techniques, along with discussion of advantages of ultrasound in tissue engineering. Subsequent sections then provide descriptions of conventional B-scan ultrasound imaging, quantitative ultrasound techniques, and elastography, with numerous representative examples of how these ultrasound-based techniques can be employed as non-invasive, non-destructive tools for tissue engineering and biomaterials fabrication.

OVERVIEW OF ULTRASOUND IMAGING AND ITS ADVANTAGES

Ultrasound describes sound fields at frequencies higher than the audible range of the human ear (i.e., > 20 kHz). Clinical ultrasound imaging utilizes sound pressure waves, with frequencies nominally ranging from 1 to 15 MHz, to generate images of structural features in biological tissue. Ultrasound imaging has advantages as an imaging modality because it is non-destructive, non-ionizing, has a penetration depth of several centimeters, and can provide real-time assessment of large, 3-D tissue volumes. The frequency of the ultrasound wave can be tuned to adjust both the penetration depth and the spatial resolution of ultrasound images for various applications, from imaging relatively small tissue constructs to large organs. As a noninvasive imaging tool, ultrasound can be easily incorporated into sterile environments necessary for tissue engineering and biomaterials fabrication protocols. Furthermore, ultrasound is rapid and non-destructive, thereby providing an excellent imaging approach for longitudinal monitoring of engineered constructs over time. Lastly, because ultrasound propagates through tissue as a focused beam, it can be used to image and monitor the development of engineered constructs after implantation in the body.

Ultrasound transducers can range from single-element, piezoelectric sources to complex, electronic arrays that provide dynamic focusing and scanning capabilities. In typical ultrasound imaging techniques, an ultrasound source emits short pulses of ultrasound that propagate through the material of interest. Scattering and reflection of ultrasound energy occurs as the acoustic wave interacts with structures of different acoustic impedances. Specular reflection occurs when the structure is large relative to the ultrasound wavelength. In comparison, when structures are much smaller than the ultrasound wavelength, diffusive or diffractive scattering can occur leading to scattering of the ultrasound energy in multiple directions. Backscattered echoes generated within the material by reflections and scattering are then received by the ultrasound transducer as a function of time. The depth of each echo can be calculated by knowledge of the speed of sound in the material and time-of-flight of each received echo.

Ultrasound imaging has several imaging modes including A-scan, B-scan, and C-scan (Figure 1A). A-scan imaging (A-mode) displays the one-dimensional (1-D) voltage amplitude of the received ultrasound radiofrequency (RF), backscattered echoes as a function of time. This 1-D signal of echoes from a single propagation path is commonly called an A-line or an RF line (Figure 1B). B-scan imaging (B-mode) provides two-dimensional (2-D) gray-scale images, and is the most common imaging mode used in clinical diagnostic ultrasound. B-mode provides visualization of imaging planes that are

parallel to the direction of sound propagation (Figure 1A). A B-scan image can be created by translating a single-element transducer, calculating the envelope of received RF lines stacked in the lateral direction, and displaying the amplitude of the envelope in gray-scale. Commercial ultrasound scanners typically use linear or phased array transducers to simultaneously scan and display an imaging plane. In comparison, C-scan imaging (C-mode) provides 2-D gray-scale images of planes that are perpendicular to the direction of sound propagation (Figure 1A). Examples of 2-D, B-scan and C-scan images of collagen hydrogels embedded with fibroblasts are shown in Figures 1C and 1D, respectively. These gray-scale images contain a speckle pattern that was produced by the interference of backscattered waves from sub-resolution scattering structures (e.g., fibroblasts) within the hydrogel. Constructive and destructive interference of scattered waves from sub-resolution scattering structures produces this speckle pattern commonly observed in B-scan images. Three-dimensional (3-D) images can be produced from a series of 2-D, B-scans that are acquired over a specific volume, and four-dimensional (4-D) imaging typically refers to 3-D ultrasound imaging in real-time. In addition, Doppler ultrasound techniques may be used to visualize fluid flow, and therefore can provide functional information on perfusion. Lastly, quantitative ultrasound and elastography techniques can provide system-independent metrics to characterize tissue or biomaterial properties to complement conventional ultrasound imaging.

High-frequency, pulse-echo ultrasound systems utilizing frequencies above that of clinical ultrasound (i.e., nominally > 20 MHz) have been developed to achieve imaging resolutions on the order of tens of microns.[4] High-frequency ultrasound can provide images of tissues noninvasively with microscopic resolution at penetration depths often inaccessible to optical-based methods.[5] High-frequency ultrasound has been investigated in a variety of clinical applications in native tissues, including opthalmology, dermatology, and cardiology.[6-8]

Ultrasound contrast agents provide further capabilities to enhance ultrasound imaging techniques.[9,10] Ultrasound contrast agents are gas-filled microbubbles that are stabilized by protein, lipid, or polymer shells. Microbubbles on the order of 1-10 μm in diameter are used clinically as contrast agents to enhance ultrasound backscatter to improve diagnostic imaging. Innovative imaging modalities that depend on unique interactions of the ultrasound field with the microbubbles have been developed specifically for the use of ultrasound contrast agents. Such contrast-based imaging modalities include harmonic imaging, sub-harmonic imaging, coded excitation, and phase-inversion imaging, among others.[9,10] Targeted contrast agents contain specific ligands on the bubble surface to provide site-specific localization of microbubbles to cells, proteins, or other biomaterials.[9] These targeted contrast agents can expand the capabilities of ultrasound to site-specific cellular and molecular imaging.[9,11] It should be noted that the interaction of ultrasound and microbubble contrast agents can lead to acoustic cavitation, which may pose potential adverse effects on engineered tissues and biomaterials. Acoustic cavitation can produce localized heat generation, fluid streaming, and shear forces.[12,13] In general, the extent of cavitation can be reduced by use of higher ultrasound frequencies, lower pressure amplitudes, shorter pulse durations, and lower concentrations of microbubbles.[12,13]

In summary, ultrasound provides numerous imaging modalities for visualizing tissue structures in real-time, and is established as an indispensible tool for diagnostic clinical imaging. Now, ultrasound imaging techniques are providing new enabling technologies to advance the field of tissue engineering. The following three sections review representative examples that demonstrate the capabilities of conventional B-mode scanning, quantitative ultrasound imaging techniques, and elastography for tissue engineering and biomaterials fabrication processes.

B-MODE ULTRASOUND IMAGING

B-mode ultrasound imaging offers the capability for real-time, non-invasive, and nondestructive visualization of engineered tissues and biomaterials. Conventional B-mode imaging typically employs frequencies in the ~1-15 MHz frequency range. B-mode ultrasound imaging provides a valuable tool for monitoring tissue structure and biomaterials fabrication processes in vitro and in vivo. For example, B-mode ultrasound imaging (12 MHz) has been employed to visualize in situ-forming drug delivery implants comprised of poly(lactic-co-glycolic)acid (PLGA).[14] Analyses of the mean gray-scale values of images, both in vitro and in vivo, demonstrated the utility of this approach to noninvasively monitor the phase inversion process and rate of drug release from the implants.[14] Another group[15] used B-scan ultrasound (13 MHz) to image fibrin gels embedded with myofibroblasts over an 18-day period, and demonstrated a linear correlation of mean gray-scale values with hydroxyproline content within the hydrogel.

High-frequency ultrasound imaging (nominally > 20 MHz) offers improved spatial resolution (~10-100 μm) for imaging engineered constructs and biomaterials, and has been used to image tissue microstructures (e.g., cells and cell nuclei) in vitro. Although the attenuation of ultrasound increases with increasing frequency, thereby decreasing the depth of penetration, high-frequency ultrasound can still provide volumetric imaging capabilities within hydrogel-based constructs. For example, high-frequency (38 MHz) B-scan imaging of cell-embedded hydrogels has been employed to visualize differences in cell concentration, observed as differences in echogenicity[16,17] (Figure 2). Additionally, high-frequency B-scan imaging (38 MHz) can provide the capability for visualizing regional variations in cell or microparticle concentration volumetrically within hydrogel constructs in vitro (Figure 1C). Although high-frequency ultrasound can not resolve individual collagen fiber microstructure, increasing echogenicity of high-frequency B-scan images of collagen hydrogels correlates with increasing collagen concentration or decreasing polymerization temperature.[18] Acoustic microscopy techniques (at 61 MHz), have been used to characterize the development and surface irregularities of engineered human oral mucosal constructs.[19,20]

Diagnostic capabilities of conventional B-scan imaging can be further improved through the use of multi-modal imaging and/or ultrasound contrast agents. In one study, three different ultrasound imaging modalities were employed to evaluate extracellular matrix scaffolds used for liver organoid formation.[21] In that study, high-frequency B-scans provided visualization of scaffold structure, dynamic contrast-enhanced imaging tracked perfusion, and microvascular structure was imaged using an ultrasound-based angiography

technique.[21] Multi-modal imaging employing high-frequency ultrasound imaging combined with time-resolved fluorescence spectroscopy has been used for nondestructive imaging and evaluation of vascular tissue grafts.[22] While high-frequency (40 MHz) ultrasound images provided information on the structure and integration of the vascular graft, fluorescence spectroscopy provided complementary information on collagen and elastin content.[22] In other studies, high-frequency ultrasound imaging and time-resolved fluorescence spectroscopy have been combined to evaluate articular cartilage constructs,[23] or to monitor changes in extracellular matrix content during chondrogenic differentiation of stem cells in hydrogels.[24] Photoacoustic imaging combined with B-scan imaging can also provide enhanced and unique capabilities for visualizing biomaterials and engineered tissues.[3,25] Photoacoustic imaging is a hydrid imaging modality that uses the absorption of pulsed laser light in tissues to produce local thermoelastic expansion leading to the generation of an ultrasound wave, which is detected by a transducer array to form an image.[26] Furthermore, the use of nanoparticle targeting agents can provide additional cellular or molecular imaging capabilities.[25,27,28] Multi-modal imaging approaches, employing dual ultrasound and photoacoustic imaging, have been used to image adipose-derived stem cells loaded with gold nanotracers embedded within fibrin hydrogels,[29] to characterize burn injury and monitor progression of an implanted engineered construct,[26] and to image and monitor blood oxygen saturation within and near PLGA-based scaffolds.[30]

Although gray-scale ultrasound images provide real-time visualization capabilities, conventional B-mode imaging does not provide quantitative metrics to characterize the structural, mechanical, and/or biological properties of biomaterials and engineered tissues. Specifically, B-scan images display only the envelope of RF echoes, and importantly, are affected by acoustic attenuation and various system-dependent parameters. Specifically, the resolution of the B-scan image is determined by the frequency response of the ultrasound system used to obtain the image. B-scan images also rely on system-dependent parameters set by the user. As examples, users can adjust various parameters, such as the electronic gain, the number of focus levels, and the size of the imaging field-of-view, to present the B-scan image to the user's preferences. These system-dependent parameters can vary between users and ultrasound systems, making it challenging to quantitatively compare B-scan images. Thus, there is a need for ultrasound imaging techniques that can provide quantitative, system-independent parameters to assess engineered tissues. These quantitative ultrasound techniques are the focus of the following section.

QUANTITATIVE ULTRASOUND

Quantitative ultrasound tissue characterization encompasses a variety of signal processing and measurement techniques designed to extract information from RF ultrasound echo signals. Quantitative ultrasound can differentiate between healthy and diseased tissues, and monitor changes in tissue properties over time, by providing quantitative metrics that estimate tissue properties, independent of ultrasound system and user settings.[31-33] These quantitative ultrasound tissue parameters can be classified into two groups based on how they are extracted from the backscattered RF signals in either the time or frequency domain. One group is derived by analyzing the amplitude of the RF echo signals, and these parameters include the speed of sound[34] and the nonlinearity parameter.[35] A second group is

comprised of parameters that can be extracted from the power spectrum of the backscattered RF signals. These frequency-dependent parameters include the midband fit,[36,37] spectral intercept,[37] spectral slope,[33,37] backscatter coefficient,[33,38] effective scatterer diameter,[38] and integrated backscatter coefficient (IBC).[34,39,40] The absorption and attenuation coefficients of materials can be measured by analyzing either the amplitude or the frequency spectrum of the backscattered RF signals. In comparison to qualitative B-scan imaging, quantitative ultrasound techniques are independent of the ultrasound device, system settings, and user. As such, these techniques provide capabilities for quantitative monitoring of structural, biological, and/or mechanical properties of engineered constructs over time, as well as for quantitative comparisons of tissue metrics between different ultrasound devices and/or user settings.

Quantitative ultrasound techniques have been applied to a broad range of native tissues, such as liver, pancreas, prostate, eyes, heart, and lymph nodes.[31,41-43] In native tissues, quantitative ultrasound techniques have been used to characterize tumors,[43] monitor cell death,[37,44] assess cardiac abnormalities,[45] characterize ultrasound contrast agents,[46] and evaluate therapeutic responses of diseased tissues after treatments with high intensity focused ultrasound or chemotherapeutic agents.[38,47,48] Furthermore, employing high-frequency ultrasound increases the backscatter coefficient of sub-resolution scatterers in tissues, such as cells and collagen fibers. High-frequency ultrasound has been employed to investigate the backscatter coefficient of blood during clotting,[39] to assess backscatter properties of cells and isolated nuclei,[34,49] to characterize human dermis,[39,50] and to monitor cell death in vitro.[51,52]

Attenuation, absorption, and the speed of sound are all acoustic parameters that can be employed as metrics to quantify properties of tissues and biomaterials. Several methodologies can be used to measure the speed of sound, the simplest of which is to measure the thickness of the material and then divide that by the time it takes for an ultrasound pulse to propagate through that thickness of the material using either through-transmission or reflection techniques. As an example, in one study, the speed of sound was measured in agarose hydrogels at concentrations ranging from 1-10%.[53] Speed of sound measurements were then used to estimate the moduli of these hydrogels using both elastic and poroelastic models.[53]

Acoustic attenuation describes the loss of amplitude of an acoustic field as it propagates through a material. Attenuation is comprised of contributions from both scattering and absorption (i.e., the conversion of ultrasound energy to heat). Attenuation is typically measured using insertion-loss techniques, while the ultrasound absorption of a material can be obtained through direct measurement of ultrasound-induced heating using thermocouple techniques. One study that employed attenuation as a metric of tissue properties demonstrated that the amplitude of an ultrasound pulse transmitted through bone marrow stromal cell/β-tricalcium phosphate composites could be correlated with the number of cells within the construct.[54] Furthermore, the dependence of the absorption coefficient on acoustic frequency can also be employed to characterize tissues and materials. The frequency-dependent attenuation coefficients of collagen hydrogels were measured using through-transmission insertion loss techniques for various concentrations of collagen.[18]

Power-law fits of the attenuation coefficients over a high-frequency band of ~15-45 MHz demonstrated the use of ultrasound to noninvasively detect and quantify difference in collagen concentration.[18] Another group measured both the speed of sound and the frequency dependence of the attenuation of constructs composed of chondrocytes embedded in poly(ethylene glycol) hydrogels, and tested these parameters as metrics to quantify hydrogel degradation over a period of several weeks.[55] Scanning acoustic microscopy (SAM) uses very high frequency ultrasound (typically > 100 MHz), and has been employed to image and quantify speed of sound and attenuation in tissue-engineered cartilage constructs.[56]

Quantitative ultrasound techniques are also finding applications for monitoring dental implant procedures, and assessing musculoskeletal engineered tissues. The stability of a dental implant within bone, and the associated soft tissue healing, are both critical for the success of implant procedures. One group employed a quantitative ultrasound metric derived from the amplitudes of echoes received from a 10-MHz ultrasound pulse propagating within a dental implant to assess implant stability in vitro and osseointegration in vivo.[57,58] Another group employed a similar time-domain analysis of 10-MHz RF echoes, combined with wavelet transformation analyses, to assess the integration of tissue-engineered cartilage.[59]

Ultrasound backscatter provides the basis for several other quantitative ultrasound parameters that have been employed to characterize tissues. Quantitative ultrasound techniques that extract spectral parameters from the backscatter RF signals can be used to characterize tissue microstructure, such as the number, size, and organization of tissue scatterers.[33,36,60] Ultrasound backscatter amplitudes depend on the concentration, size, density, and compressibility of sub-resolution scatterers.[33,36,60] The integrated backscatter coefficient (IBC) is a system-independent parameter that estimates the backscatter strength of sub-resolution scatterers per unit volume over the transducer bandwidth.[33,36] Recent studies have shown that backscatter spectral techniques can provide important tools for the field of tissue engineering, as illustrated with the following examples.

A recent study developed the use of high-frequency quantitative ultrasound to nondestructively estimate cell concentration in 3-D hydrogels.[16] IBCs were computed from high-frequency (13-47 MHz) backscatter RF measurements obtained from agarose hydrogels embedded with fibroblasts.[16] The IBC increased linearly with increasing cell concentrations from 5×10^4 to 1×10^6 cells/mL.[16] Furthermore, the technique can be used to generate color-scaled parametric images of cell concentration as a tool to visualize spatial variations in cell concentration in 3-D hydrogels volumetrically.[16]

The IBC has also been used to detect and quantify changes in collagen fiber density and diameter in hydrogels fabricated with different collagen concentrations or under different polymerization temperatures.[18] Parametric images of the IBC provided the capability of visualizing regional variations in collagen fiber microstructure.[18] In contrast to second harmonic generation imaging or scanning electron microscopy, this high-frequency IBC technique provides for visualization of backscatter from collagen structures in thick (~1 cm) hydrogels. In this study, parametric images were generated with axial resolutions of 41 μm

and lateral resolutions of 850 μm.[18] Images can be generated in either B-scan or C-scan planes (Figure 3) or combined for volumetric imaging.

Other spectral parameters, including the spectral slope and midband fit, are also useful metrics to quantitatively characterize engineered tissues and biomaterials. Although the techniques do not image individual cells, the midband fit, spectral slope, and high-frequency signal statistics can detect apoptosis and monitor cell viability.[37,49,61] In one study, high-frequency ultrasound was employed for 3-D gray-scale imaging of collagen-based constructs, and quantitative spectral parameters, namely the spectral slope and midband fit, were used to characterize the mineral (i.e., hydroxyapatite) content of the constructs.[62] In this study, the midband fit correlated with hydroxyapatite content and calcium deposition.[62] Another study employed combined measurements of speed of sound, attenuation, midband fit, and spectral slope to characterize osteoblastic differentiation within 3-D collagen hydrogels.[63] High-frequency spectral ultrasound estimation of cell diameter, cell concentration, and calcium content within these constructs was in good agreement with biochemical assay results.[63]

ELASTOGRAPHY

The mechanical environment of engineered tissues can influence cellular functions that are important for tissue regeneration, including cell migration, proliferation, and differentiation.[64,65] Direct mechanical tests are destructive, and thus, do not facilitate monitoring changes in mechanical properties of individual engineered tissue constructs over time or in vivo. Furthermore, direct mechanical tests provide only bulk measurements of the mechanical properties and do not enable measurements at localized regions within tissue samples. To overcome these limitations, ultrasound elastography is emerging as a valuable technique for tissue engineering applications.

Ultrasound elastography describes a variety of techniques to image the viscoelastic properties of tissues and materials non-destructively and non-invasively.[66,67] Numerous ultrasound elastography techniques are under development, differing in their methods used to generate tissue motion and detect resulting displacements.[66,67] Quasi-static elastography techniques, sometimes termed compression elastography, apply small compressions in the tissue sample and then track axial components of displacement using B-scan imaging.[66] Dynamic elastography approaches use transient or harmonic sources to produce shear waves in tissue. The resultant tissue displacements are then tracked with various diagnostic imaging techniques and can provide estimates of the shear modulus of the tissue.[66,67] Several dynamic elastography techniques include vibration amplitude sonoelasticity imaging,[68] transient shear wave elastography,[67] crawling wave elastography,[69] and acoustic radiation force elastography[70]. Some of these techniques have been used clinically to assess liver stiffness in patients with hepatitis,[71] to differentiate between benign and malignant lesions in breast cancer patients, and to aid in detecting areas of prostate cancer[72].

For tissue engineering applications, most investigations thus far have employed compression elastography techniques to obtain relative measurements of the mechanical properties of engineered tissues.[73-76] One study demonstrated the use of a compression elastography

technique to compute the relative strain of thin, polyglycolic acid (PGA) scaffolds, embedded with smooth muscle cells.[76] Another study used compression elastography techniques to generate axial strain images for monitoring the degradation of biodegradable, polymer-based scaffolds embedded in gelatin phantoms or implanted subcutaneously in mouse models[74]. Similarly, compression elastography was able to track changes in mechanical stiffness of polyurethane scaffolds implanted in a mouse model over a 12-week period.[73] Quasi-static elastography was also employed to monitor the modulus of engineered arterial constructs during fabrication, where displacements were induced by pulsatile flow within the constructs.[75] In general, compression elastography techniques provide only relative estimates of the elastic properties of tissues because the applied stress field is typically not known.[66] Furthermore, compression elastography techniques typically require direct contact with the tissue or biomaterial to produce compression, and in vivo applications are limited to superficial tissues.

Elastography techniques are also finding applications for characterizing relatively hard tissues, including bone and bone substitute materials. Compression elastography has been demonstrated capable of visualizing differences in elastic properties of polymer samples with moduli ranging from 47 kPa to 4 MPa.[77] Other ultrasound techniques, have been employed to characterize the properties of porous baghdadite scaffolds[78] or bioglass-based scaffolds[79] used for bone tissue engineering. In these studies, pulse-echo ultrasound was used to measure the time-of-flight, estimate the longitudinal wave velocity, and then calculate the normal component of the stiffness tensor. The normal component of the stiffness decreased monotonically with increasing biomaterial porosity.[78] However, this ultrasound technique does not provide quantitative measurement of the modulus of materials.

In comparison to compression elastography, acoustic radiation force elastography techniques induce tissue deformation site-specifically, and then monitor the resulting shear wave to estimate the shear modulus of the tissue.[66,67] Acoustic radiation force elastography techniques utilize a focused ultrasound beam to generate an acoustic radiation force in order to induce local tissue displacements.[66,67] Acoustic radiation force is a body force generated by a transfer of momentum from the acoustic field to the tissue.[80] In acoustic radiation force elastography, a high-intensity (~1 kW/cm^2) ultrasound pulse (on the order of 100-μs durations) is typically used to create the acoustic radiation force, resulting in tissue displacements of ~1-20 μm.[67,70,81] After application of the radiation force, tissue deformation (i.e., displacement) associated with shear wave propagation is monitored spatially over time using conventional pulse-echo ultrasound.[67,70,81] Several acoustic radiation force elastography techniques have been developed, each implementing different methods to apply the radiation force or track the resultant shear wave.[67,70,82] These techniques include acoustic radiation force impulse (ARFI) imaging,[70] spatially modulated ultrasound radiation force (SMURF),[83] shear wave elasticity imaging (SWEI),[67] acoustic vibroacoustography,[84] shear wave dispersion ultrasonic velocity (SDUV),[85] single tracking location acoustic radiation force impulse (STL-ARFI) imaging[82], and supersonic shear wave imaging[86].

Acoustic radiation force elastography techniques are finding new applications for characterizing 3-D engineered tissues because of their ability to provide quantitative estimates of the mechanical properties of tissues site-specifically, volumetrically, rapidly, and non-destructively. Furthermore, acoustic radiation force elastography techniques do not require contact with the tissue, which is important for sterile tissue engineering environments. Shear moduli of tissue phantoms were estimated using SMURF techniques and found to be in good agreement with measurements of moduli using destructive mechanical testing techniques.[87] Another study employed single tracking location shear wave elasticity imaging for estimating shear moduli of cell-embedded collagen hydrogels.[88] Of note, this study also demonstrated that the generation of Scholte surface waves can confound the estimation of moduli near fluid-solid interfaces, as may occur when imaging engineered constructs within standard tissue culture plates.[88] Acoustic radiation force techniques were also used to image tissue displacements in thin tissue constructs.[89] Moreover, acoustic radiation force elastography techniques can image deeper tissue regions than compression elastography, thereby enabling assessment of engineered tissues implanted in vivo. As an example, one study employed a multi-modal imaging approach to monitor mechanical and structural changes in degradable, polymer scaffolds implanted in rats in vivo (Figure 4).[90] Acoustic radiation force shear wave imaging was employed to estimate shear moduli, and photoacoustic imaging was used for structural imaging of the scaffolds.[90] Changes in shear modulus of scaffolds implanted in vivo measured with shear wave imaging correlated with Young's moduli obtained by compression testing ex vivo.[90]

SUMMARY

In summary, ultrasound offers unique capabilities for real-time imaging and quantitative monitoring of various properties of engineered tissues and biomaterials in vitro and in vivo. Conventional ultrasound B-scan imaging offers rapid, non-destructive imaging, and diagnostic information can be improved when combined with other imaging modalities or with the use of contrast agents. High-frequency quantitative ultrasound techniques, including elastography, provide metrics for quantitative assessment of structural, biological, and mechanical properties of engineered constructs. Ultrasound imaging and quantitative characterization techniques can offer new enabling techniques for tissue engineering, and can complement other imaging modalities. Avenues for future research to advance quantitative ultrasound techniques include; developing acoustic scattering models to characterize engineered constructs comprised of multiple cell types and extracellular matrix components, combining multiple quantitative metrics to characterize complex engineered tissues, validating techniques broadly across multiple tissue types, and meeting challenges associated with in vivo translation. Overall, advancing ultrasound technologies in tissue engineering will facilitate volumetric, non-invasive, and non-destructive evaluation of engineered constructs during fabrication, conditioning, and post-implantation, thus allowing for functional comparisons among different approaches, and accelerating clinical translation.

ACKNOWLEDGEMENTS

This work was supported, in part, by a grant from the National Institutes of Health (R01 EB018210).

REFERENCES

1. Atala A. Engineering organs. Curr Opin Biotechnol. 2009; 20:575–592. [PubMed: 19896823]
2. Appel AA, Anastasio MA, Larson JC, Brey EM. Imaging challenges in biomaterials and tissue engineering. Biomaterials. 2013; 34:6615–6630. [PubMed: 23768903]
3. Nam SY, Ricles LM, Suggs LJ, Emelianov SY. Imaging strategies for tissue engineering applications. Tissue Eng Part B Rev. 2015; 21:88–102. [PubMed: 25012069]
4. Foster FS, Pavlin CJ, Harasiewicz KA, Christopher DA, Turnbull DH. Advances in ultrasound biomicroscopy. Ultrasound Med Biol. 2000; 26:1–27. [PubMed: 10687788]
5. Sherar MD, Starkoski BG, Taylor WB, Foster FS. A 100 MHz B-scan ultrasound backscatter microscope. Ultrason Imaging. 1989; 11:95–105. [PubMed: 2660392]
6. Pavlin CJ, Harasiewicz K, Sherar MD, Foster FS. Clinical use of ultrasound biomicroscopy. Ophthalmology. 1991; 98:287–295. [PubMed: 2023747]
7. Potkin BN, Bartorelli AL, Gessert JM, Neville RF, Almagor Y, Roberts WC, Leon MB. Coronary artery imaging with intravascular high-frequency ultrasound. Circulation. 1990; 81:1575–1585. [PubMed: 2184946]
8. Hoffmann K, Jung J, el Gammal S, Altmeyer P. Malignant melanoma in 20-MHz B scan sonography. Dermatology. 1992; 185:49–55. [PubMed: 1638071]
9. Ferrara K, Pollard R, Borden M. Ultrasound microbubble contrast agents: fundamentals and application to gene and drug delivery. Annu Rev Biomed Eng. 2007; 9:415–447. [PubMed: 17651012]
10. Qin S, Caskey CF, Ferrara KW. Ultrasound contrast microbubbles in imaging and therapy: physical principles and engineering. Phys Med Biol. 2009; 54:R27–57. [PubMed: 19229096]
11. Gessner R, Dayton PA. Advances in molecular imaging with ultrasound. Mol Imaging. 2010; 9:117–127. [PubMed: 20487678]
12. Nyborg W. WFUMB Safety Symposium on Echo-Contrast Agents: mechanisms for the interaction of ultrasound. Ultrasound Med Biol. 2007; 33:224–232. [PubMed: 17223251]
13. Dalecki D. WFUMB Safety Symposium on Echo-Contrast Agents: bioeffects of ultrasound contrast agents in vivo. Ultrasound Med Biol. 2007; 33:205–213. [PubMed: 17239521]
14. Solorio L, Babin BM, Patel RB, Mach J, Azar N, Exner AA. Noninvasive characterization of in situ forming implants using diagnostic ultrasound. J Control Release. 2010; 143:183–190. [PubMed: 20060859]
15. Kreitz S, Dohmen G, Hasken S, Schmitz-Rode T, Mela P, Jockenhoevel S. Nondestructive method to evaluate the collagen content of fibrin-based tissue engineered structures via ultrasound. Tissue Eng Part C Methods. 2011; 17:1021–1026. [PubMed: 21663456]
16. Mercado KP, Helguera M, Hocking DC, Dalecki D. Estimating cell concentration in three-dimensional engineered tissues using high frequency quantitative ultrasound. Ann Biomed Eng. 2014; 42:1292–1304. [PubMed: 24627179]
17. Inkinen S, Liukkonen J, Ylarinne JH, Puhakka PH, Lammi MJ, Viren T, Jurvelin JS, Toyras J. Collagen and chondrocyte concentrations control ultrasound scattering in agarose scaffolds. Ultrasound Med Biol. 2014; 40:2162–2171. [PubMed: 24972499]
18. Mercado KP, Helguera M, Hocking DC, Dalecki D. Noninvasive Quantitative Imaging of Collagen Microstructure in Three-Dimensional Hydrogels Using High-Frequency Ultrasound. Tissue Eng Part C Methods. 2015
19. Winterroth F, Hollman KW, Kuo S, Izumi K, Feinberg SE, Hollister SJ, Fowlkes JB. Comparison of scanning acoustic microscopy and histology images in characterizing surface irregularities among engineered human oral mucosal tissues. Ultrasound Med Biol. 2011; 37:1734–1742. [PubMed: 21871704]
20. Winterroth F, Lee J, Kuo S, Fowlkes JB, Feinberg SE, Hollister SJ, Hollman KW. Acoustic microscopy analyses to determine good vs. failed tissue engineered oral mucosa under normal or thermally stressed culture conditions. Ann Biomed Eng. 2011; 39:44–52. [PubMed: 20924679]
21. Gessner RC, Hanson AD, Feingold S, Cashion AT, Corcimaru A, Wu BT, Mullins CR, Aylward SR, Reid LM, Dayton PA. Functional ultrasound imaging for assessment of extracellular matrix

scaffolds used for liver organoid formation. Biomaterials. 2013; 34:9341–9351. [PubMed: 24011714]

22. Fatakdawala H, Griffiths LG, Humphrey S, Marcu L. Time-resolved fluorescence spectroscopy and ultrasound backscatter microscopy for nondestructive evaluation of vascular grafts. J Biomed Opt. 2014; 19:080503. [PubMed: 25147960]
23. Sun Y, Responte D, Xie H, Liu J, Fatakdawala H, Hu J, Athanasiou KA, Marcu L. Nondestructive evaluation of tissue engineered articular cartilage using time-resolved fluorescence spectroscopy and ultrasound backscatter microscopy. Tissue Eng Part C Methods. 2012; 18:215–226. [PubMed: 22010819]
24. Fite BZ, Decaris M, Sun Y, Lam A, Ho CK, Leach JK, Marcu L. Noninvasive multimodal evaluation of bioengineered cartilage constructs combining time-resolved fluorescence and ultrasound imaging. Tissue Eng Part C Methods. 2011; 17:495–504. [PubMed: 21303258]
25. Emelianov SY, Li PC, O'Donnell M. Photoacoustics for molecular imaging and therapy. Phys Today. 2009; 62:34–39. [PubMed: 20523758]
26. Nam SY, Chung E, Suggs LJ, Emelianov SY. Combined ultrasound and photoacoustic imaging to noninvasively assess burn injury and selectively monitor a regenerative tissue-engineered construct. Tissue Eng Part C Methods. 2015; 21:557–566. [PubMed: 25384558]
27. Mallidi S, Kim S, Karpiouk A, Joshi PP, Sokolov K, Emelianov S. Visualization of molecular composition and functionality of cancer cells using nanoparticle-augmented ultrasound-guided photoacoustics. Photoacoustics. 2015; 3:26–34. [PubMed: 25893171]
28. Wilson K, Homan K, Emelianov S. Biomedical photoacoustics beyond thermal expansion using triggered nanodroplet vaporization for contrast-enhanced imaging. Nat Commun. 2012; 3:618. [PubMed: 22233628]
29. Chung E, Nam SY, Ricles LM, Emelianov SY, Suggs LJ. Evaluation of gold nanotracers to track adipose-derived stem cells in a PEGylated fibrin gel for dermal tissue engineering applications. Int J Nanomedicine. 2013; 8:325–336. [PubMed: 23345978]
30. Talukdar Y, Avti P, Sun J, Sitharaman B. Multimodal ultrasoundphotoacoustic imaging of tissue engineering scaffolds and blood oxygen saturation in and around the scaffolds. Tissue Eng Part C Methods. 2014; 20:440–449. [PubMed: 24107069]
31. Lizzi FL, Greenebaum M, Feleppa EJ, Elbaum M, Coleman DJ. Theoretical framework for spectrum analysis in ultrasonic tissue characterization. J Acoust Soc Am. 1983; 73:1366–1373. [PubMed: 6853848]
32. Insana MF, Hall TJ. Characterising the microstructure of random media using ultrasound. Phys Med Biol. 1990; 35:1373–1386. [PubMed: 2243842]
33. Insana MF, Wagner RF, Brown DG, Hall TJ. Describing small-scale structure in random media using pulse-echo ultrasound. J Acoust Soc Am. 1990; 87:179–192. [PubMed: 2299033]
34. Taggart LR, Baddour RE, Giles A, Czarnota GJ, Kolios MC. Ultrasonic characterization of whole cells and isolated nuclei. Ultrasound Med Biol. 2007; 33:389–401. [PubMed: 17257739]
35. Zhang D, Gong X, Ye S. Acoustic nonlinearity parameter tomography for biological specimens via measurements of the second harmonics. J Acoust Soc Am. 1996; 99:2397–2402. [PubMed: 8730085]
36. Lizzi FL, Astor M, Feleppa EJ, Shao M, Kalisz A. Statistical framework for ultrasonic spectral parameter imaging. Ultrasound Med Biol. 1997; 23:1371–1382. [PubMed: 9428136]
37. Kolios MC, Czarnota GJ, Lee M, Hunt JW, Sherar MD. Ultrasonic spectral parameter characterization of apoptosis. Ultrasound Med Biol. 2002; 28:589–597. [PubMed: 12079696]
38. Ghoshal G, Kemmerer JP, Karunakaran C, Abuhabsah R, Miller RJ, Sarwate S, Oelze ML. Quantitative ultrasound imaging for monitoring in situ high-intensity focused ultrasound exposure. Ultrason Imaging. 2014; 36:239–255. [PubMed: 24970857]
39. Libgot-Calle R, Ossant F, Gruel Y, Lermusiaux P, Patat F. High frequency ultrasound device to investigate the acoustic properties of whole blood during coagulation. Ultrasound Med Biol. 2008; 34:252–264. [PubMed: 18077082]
40. Lebertre M, Ossant F, Vaillant L, Diridollou S, Patat F. Spatial variation of acoustic parameters in human skin: an in vitro study between 22 and 45 MHz. Ultrasound Med Biol. 2002; 28:599–615. [PubMed: 12079697]

41. Insana MF, Hall TJ. A method for characterizing soft tissue microstructure using parametric ultrasound imaging. Prog Clin Biol Res. 1991; 363:241–256. [PubMed: 1988977]
42. Mamou J, Coron A, Oelze ML, Saegusa-Beecroft E, Hata M, Lee P, Machi J, Yanagihara E, Laugier P, Feleppa EJ. Three-dimensional high-frequency backscatter and envelope quantification of cancerous human lymph nodes. Ultrasound Med Biol. 2011; 37:345–357. [PubMed: 21316559]
43. Lizzi F OM, Feleppa E, Rorke M, Yaremko M. Relationship of ultrasonic spectral parameters to features of tissue microstructure. IEEE Trans Ultrason Ferr. 1986; 33
44. Brand S, Weiss EC, Lemor RM, Kolios MC. High frequency ultrasound tissue characterization and acoustic microscopy of intracellular changes. Ultrasound Med Biol. 2008; 34:1396–1407. [PubMed: 18439747]
45. Katouzian A, Sathyanarayana S, Baseri B, Konofagou EE, Carlier SG. Challenges in atherosclerotic plaque characterization with intravascular ultrasound (IVUS): From data collection to classification. Ieee Transactions on Information Technology in Biomedicine. 2008; 12:315–327. [PubMed: 18693499]
46. Leithem SM, Lavarello RJ, O'Brien WD Jr. Oelze ML. Estimating concentration of ultrasound contrast agents with backscatter coefficients: experimental and theoretical aspects. J Acoust Soc Am. 2012; 131:2295–2305. [PubMed: 22423724]
47. Vlad RM, Brand S, Giles A, Kolios MC, Czarnota GJ. Quantitative ultrasound characterization of responses to radiotherapy in cancer mouse models. Clin Cancer Res. 2009; 15:2067–2075. [PubMed: 19276277]
48. Kemmerer JP, Oelze ML. Ultrasonic assessment of thermal therapy in rat liver. Ultrasound Med Biol. 2012; 38:2130–2137. [PubMed: 23062365]
49. Tunis AS, Czarnota GJ, Giles A, Sherar MD, Hunt JW, Kolios MC. Monitoring structural changes in cells with high-frequency ultrasound signal statistics. Ultrasound Med Biol. 2005; 31:1041–1049. [PubMed: 16085095]
50. Guittet C OF, Vaillant L, Berson M. In vivo high-frequency ultrasonic characterization of human dermis. IEEE Trans Biomed Eng. 1999; 46
51. Czarnota GJ, Kolios MC, Abraham J, Portnoy M, Ottensmeyer FP, Hunt JW, Sherar MD. Ultrasound imaging of apoptosis: high-resolution non-invasive monitoring of programmed cell death in vitro, in situ and in vivo. Br J Cancer. 1999; 81:520–527. [PubMed: 10507779]
52. Vlad RM, Kolios MC, Moseley JL, Czarnota GJ, Brock KK. Evaluating the extent of cell death in 3D high frequency ultrasound by registration with whole-mount tumor histopathology. Med Phys. 2010; 37:4288–4297. [PubMed: 20879589]
53. Walker JM, Myers AM, Schluchter MD, Goldberg VM, Caplan AI, Berilla JA, Mansour JM, Welter JF. Nondestructive evaluation of hydrogel mechanical properties using ultrasound. Ann Biomed Eng. 2011; 39:2521–2530. [PubMed: 21773854]
54. Oe K, Miwa M, Nagamune K, Sakai Y, Lee SY, Niikura T, Iwakura T, Hasegawa T, Shibanuma N, Hata Y, Kuroda R, Kurosaka M. Nondestructive evaluation of cell numbers in bone marrow stromal cell/beta-tricalcium phosphate composites using ultrasound. Tissue Eng Part C Methods. 2010; 16:347–353. [PubMed: 19580422]
55. Rice MA, Waters KR, Anseth KS. Ultrasound monitoring of cartilaginous matrix evolution in degradable PEG hydrogels. Acta Biomater. 2009; 5:152–161. [PubMed: 18793879]
56. Tanaka Y, Saijo Y, Fujihara Y, Yamaoka H, Nishizawa S, Nagata S, Ogasawara T, Asawa Y, Takato T, Hoshi K. Evaluation of the implant type tissue-engineered cartilage by scanning acoustic microscopy. J Biosci Bioeng. 2012; 113:252–257. [PubMed: 22138383]
57. Vayron R, Soffer E, Anagnostou F, Haiat G. Ultrasonic evaluation of dental implant osseointegration. J Biomech. 2014; 47:3562–3568. [PubMed: 25262877]
58. Mathieu V, Anagnostou F, Soffer E, Haiat G. Ultrasonic evaluation of dental implant biomechanical stability: an in vitro study. Ultrasound Med Biol. 2011; 37:262–270. [PubMed: 21257090]
59. Hattori K, Takakura Y, Ohgushi H, Habata T, Uematsu K, Ikeuchi K. Novel ultrasonic evaluation of tissue-engineered cartilage for large osteochondral defects--non-invasive judgment of tissue-engineered cartilage. J Orthop Res. 2005; 23:1179–1183. [PubMed: 15925475]

60. Lizzi FL, Astor M, Liu T, Deng C, Coleman DJ, Silverman RH. Ultrasonic spectrum analysis for tissue assays and therapy evaluation. International Journal of Imaging Systems and Technology. 1997; 8:3–10.
61. Lizzi FL, Astor M, Feleppa EJ, Shao M, Kalisz A. Statistical framework for ultrasonic spectral parameter imaging. Ultrasound in Medicine and Biology. 1997; 23:1371–1382. [PubMed: 9428136]
62. Gudur M, Rao RR, Hsiao YS, Peterson AW, Deng CX, Stegemann JP. Noninvasive, quantitative, spatiotemporal characterization of mineralization in three-dimensional collagen hydrogels using high-resolution spectral ultrasound imaging. Tissue Eng Part C Methods. 2012; 18:935–946. [PubMed: 22624791]
63. Gudur MS, Rao RR, Peterson AW, Caldwell DJ, Stegemann JP, Deng CX. Noninvasive quantification of in vitro osteoblastic differentiation in 3D engineered tissue constructs using spectral ultrasound imaging. PLoS One. 2014; 9:e85749. [PubMed: 24465680]
64. Discher DE, Janmey P, Wang YL. Tissue cells feel and respond to the stiffness of their substrate. Science. 2005; 310:1139–1143. [PubMed: 16293750]
65. Miron-Mendoza M, Seemann J, Grinnell F. The differential regulation of cell motile activity through matrix stiffness and porosity in three dimensional collagen matrices. Biomaterials. 2010; 31:6425–6435. [PubMed: 20537378]
66. Parker KJ, Doyley MM, Rubens DJ. Imaging the elastic properties of tissue: the 20 year perspective. Phys Med Biol. 2011; 56:R1–R29. [PubMed: 21119234]
67. Sarvazyan AP, Rudenko OV, Swanson SD, Fowlkes JB, Emelianov SY. Shear wave elasticity imaging: a new ultrasonic technology of medical diagnostics. Ultrasound Med Biol. 1998; 24:1419–1435. [PubMed: 10385964]
68. Lerner RM, Huang SR, Parker KJ. “Sonoelasticity” images derived from ultrasound signals in mechanically vibrated tissues. Ultrasound Med Biol. 1990; 16:231–239. [PubMed: 1694603]
69. Wu Z, Taylor LS, Rubens DJ, Parker KJ. Sonoelastographic imaging of interference patterns for estimation of the shear velocity of homogeneous biomaterials. Phys Med Biol. 2004; 49:911–922. [PubMed: 15104315]
70. Nightingale KR, Palmeri ML, Nightingale RW, Trahey GE. On the feasibility of remote palpation using acoustic radiation force. J Acoust Soc Am. 2001; 110:625–634. [PubMed: 11508987]
71. Wang JH, Changchien CS, Hung CH, Eng HL, Tung WC, Kee KM, Chen CH, Hu TH, Lee CM, Lu SN. FibroScan and ultrasonography in the prediction of hepatic fibrosis in patients with chronic viral hepatitis. J Gastroenterol. 2009; 44:439–446. [PubMed: 19308312]
72. Ginat DT, Destounis SV, Barr RG, Castaneda B, Strang JG, Rubens DJ. US elastography of breast and prostate lesions. Radiographics. 2009; 29:2007–2016. [PubMed: 19926759]
73. Yu J, Takanari K, Hong Y, Lee KW, Amoroso NJ, Wang Y, Wagner WR, Kim K. Non-invasive characterization of polyurethane-based tissue constructs in a rat abdominal repair model using high frequency ultrasound elasticity imaging. Biomaterials. 2013; 34:2701–2709. [PubMed: 23347836]
74. Kim K, Jeong CG, Hollister SJ. Non-invasive monitoring of tissue scaffold degradation using ultrasound elasticity imaging. Acta Biomater. 2008; 4:783–790. [PubMed: 18348913]
75. Dutta D, Lee KW, Allen RA, Wang Y, Brigham JC, Kim K. Non-invasive assessment of elastic modulus of arterial constructs during cell culture using ultrasound elasticity imaging. Ultrasound Med Biol. 2013; 39:2103–2115. [PubMed: 23932282]
76. Abraham Cohn N KB, Erkamp RQ, Mooney DJ, Emelianov SY, Skovoroda AR, O'Donnell M. High-resolution elasticity imaging for tissue engineering. IEEE Trans Ultrason Ferr. 2000; 47
77. Zhou H, Goss M, Hernandez C, Mansour JM, Exner A. Validation of Ultrasound Elastography Imaging for Nondestructive Characterization of Stiffer Biomaterials. Ann Biomed Eng. 2015
78. Kariem H, Pastrama MI, Roohani-Esfahani SI, Pivonka P, Zreiqat H, Hellmich C. Micro-poro-elasticity of baghdadite-based bone tissue engineering scaffolds: a unifying approach based on ultrasonics, nanoindentation, and homogenization theory. Mater Sci Eng C Mater Biol Appl. 2015; 46:553–564. [PubMed: 25492021]
79. Li W, Pastrama MI, Ding Y, Zheng K, Hellmich C, Boccaccini AR. Ultrasonic elasticity determination of 45S5 Bioglass((R))-based scaffolds: influence of polymer coating and crosslinking treatment. J Mech Behav Biomed Mater. 2014; 40:85–94. [PubMed: 25215906]

80. Rooney JA, Nyborg WL. Acoustic Radiation Pressure in a Travelling Plane-Wave. American Journal of Physics. 1972; 40:1825–&.

81. Palmeri ML, McAleavey SA, Trahey GE, Nightingale KR. Ultrasonic tracking of acoustic radiation force-induced displacements in homogeneous media. IEEE Trans Ultrason Ferroelectr Freq Control. 2006; 53:1300–1313. [PubMed: 16889337]

82. Elegbe EC, McAleavey SA. Single tracking location methods suppress speckle noise in shear wave velocity estimation. Ultrason Imaging. 2013; 35:109–125. [PubMed: 23493611]

83. McAleavey SA, Menon M, Orszulak J. Shear-modulus estimation by application of spatially-modulated impulsive acoustic radiation force. Ultrason Imaging. 2007; 29:87–104. [PubMed: 17679324]

84. Fatemi M, Greenleaf JF. Probing the dynamics of tissue at low frequencies with the radiation force of ultrasound. Phys Med Biol. 2000; 45:1449–1464. [PubMed: 10870703]

85. Chen S, Fatemi M, Greenleaf JF. Shear property characterization of viscoelastic media using vibrations induced by ultrasound radiation force. Proc. IEEE Ultrasonics Symp. 2002:1871–1875.

86. Berco J, Tanter M, Fink M. Supersonic shear imaging: a new technique for soft tissue elasticity mapping. IEEE Trans Ultrason Ferroelectr Freq Control. 2004; 51:1449–1464. [PubMed: 15600089]

87. McAleavey S, Collins E, Kelly J, Elegbe E, Menon M. Validation of SMURF estimation of shear modulus in hydrogels. Ultrason Imaging. 2009; 31:131–150. [PubMed: 19630254]

88. Mercado KP, Langdon J, Helguera M, McAleavey SA, Hocking DC, Dalecki D. Scholte wave generation during single tracking location shear wave elasticity imaging of engineered tissues. JASA Express Letters. 2015; 138

89. Liu D, Ebbini ES. Viscoelastic property measurement in thin tissue constructs using ultrasound. IEEE Trans Ultrason Ferroelectr Freq Control. 2008; 55:368–383. [PubMed: 18334343]

90. Park DW, Ye SH, Jiang HB, Dutta D, Nonaka K, Wagner WR, Kim K. In vivo monitoring of structural and mechanical changes of tissue scaffolds by multi-modality imaging. Biomaterials. 2014; 35:7851–7859. [PubMed: 24951048]

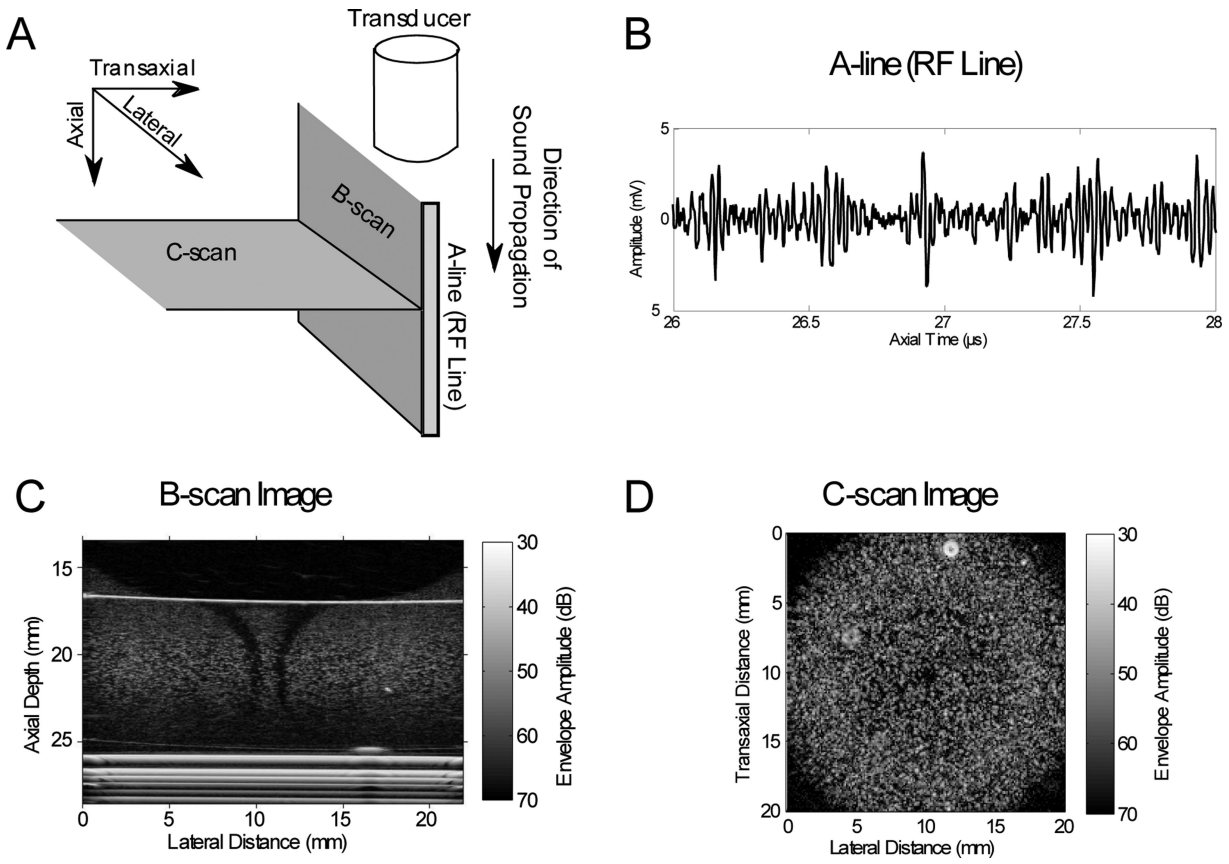

Figure 1. Ultrasound imaging modes

(A) Schematic of the orientations of common ultrasound imaging modes (i.e., A-line, B-scan, and C-scan) with respect to the direction of sound propagation. (B) A plot of an A-line (RF line) displayed as the amplitude of the backscattered ultrasound echo signal as a function of time. (C) B-scan imaging planes are parallel to the direction of sound propagation. Shown is a B-scan image of a cylindrical collagen hydrogel embedded with fibroblasts (generated using methods as described previously[16]). (D) C-scan imaging planes are perpendicular to the direction of sound propagation. Shown is a C-scan image of a cylindrical collagen hydrogel embedded with fibroblasts (generated using methods as described previously[18]).

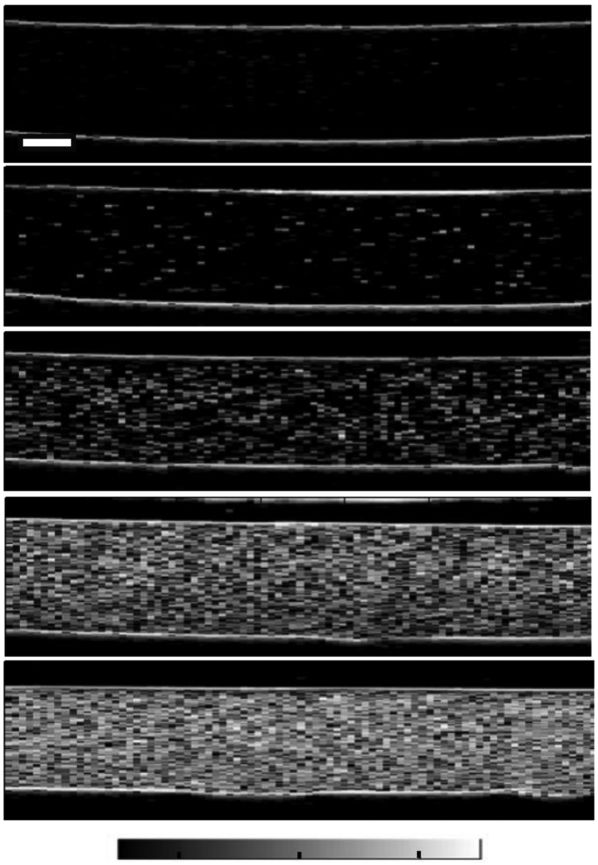

Figure 2. B-scan images of cell-embedded agarose gels

Representative agarose gels with cell concentrations of (A) 0, (B) 1×10^4, (C) 1×10^5, (D) 5×10^5, (E) 1×10^6 cell/mL. Data were acquired using a 38-MHz transducer. Scale bar, 1 mm. With kind permission from Springer Science+Business Media: Annals of Biomedical Engineering, Estimating Cell Concentration in Three-Dimensional Engineered Tissues Using High Frequency Quantitative Ultrasound, 42, 2014, 1292, Mercado, K.P., Helguera, M., Hocking, D.C., Dalecki, D. Figure 4.

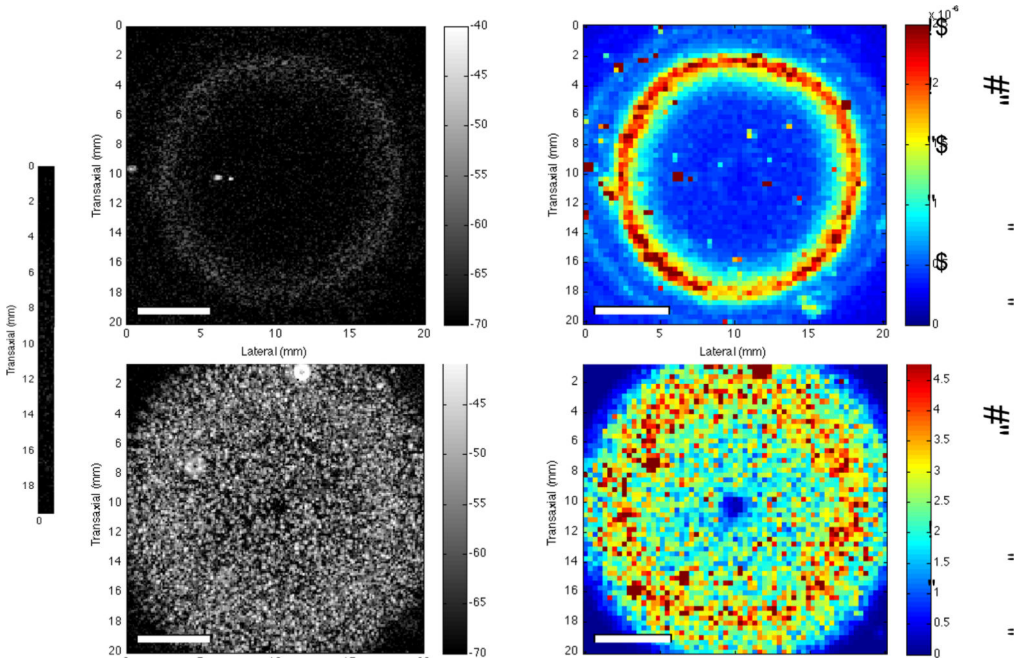

Figure 3. C-scan and IBC parametric imaging of collagen gels

Collagen (2 mg/mL) gels were fabricated in 12-well tissue culture plates in the absence (A, B) and presence (C, D) of cells. Gels were polymerized for 1 h at 37 °C. The gels were 9 mm thick and 22 mm in diameter. C-scan images of the (A) acellular and (C) cell-embedded gels are shown. The ultrasound transducer was focused at the middle of each gel (axial depth of 4.5 mm). Each pixel in the IBC images (B, D) corresponds to a 3-D ROI with 9 RF lines (3 RF lines laterally, 3 RF lines transaxially) of 1-mm axial length. Scale bar, 5 mm. Note the colorbar scale in the IBC image of cell-embedded gels (D) is an order of magnitude greater than that of acellular gels (B). Reprinted from: Tissue Engineering, Part C, Noninvasive Quantitative Imaging of Collagen Microstructure in Three-Dimensional Hydrogels Using High-Frequency Ultrasound, 21, 2015, 671, Mercado, K.P., Helguera, M., Hocking, D.C., Dalecki, D. Figure 8.

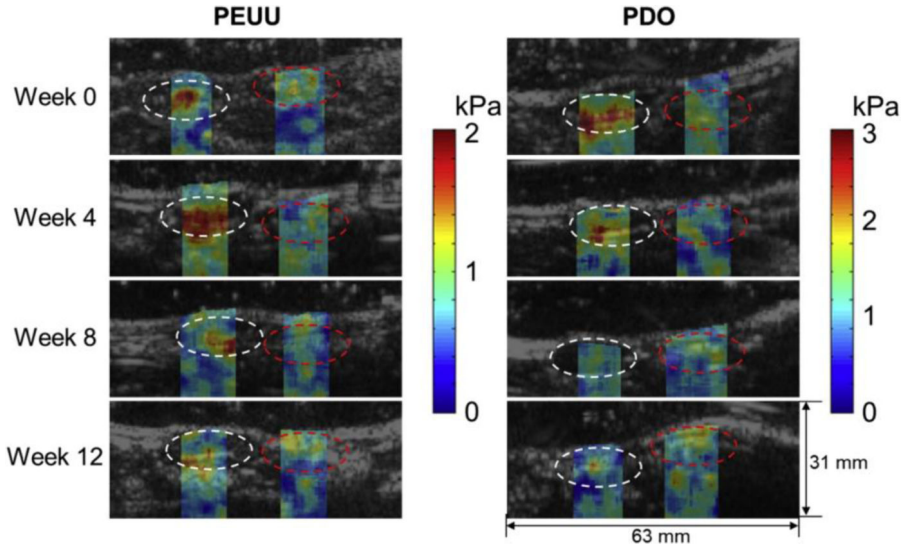

Figure 4. Elastography imaging of engineered scaffolds in vivo

Shear modulus images of degradable poly(ester urethane)urea (PEUU) and polydioxanone (PDO) scaffolds implanted in rat abdominal wall. White and red circles indicate regions of the scaffold and native abdominal wall, respectively. Reprinted from Biomaterials, 35/27, Park D.W., Ye S-H, Jiang H.B., Dutta D., Nonaka K., Wagner W.R., Kim K., In vivo monitoring of structural and mechanical changes of tissue scaffolds by multi-modality imaging, 7851, 2014, with permission from Elsevier.